Journal of Chemical&Engineering Data

pubs.acs.org/jced Article

Measurement of Optical Properties of Aqueous Lithium Bromide Solutions with and without Surfactant for Potential Use in Interferometric Analysis of Absorption Systems

Irene Pérez de Luco, Aliaksandr Mialdun,* Peru Arroiabe,* Ane Errarte,* Valentina Shevtsova,* and M. Mounir Bou-Ali*

Cite This: https://doi.org/10.1021/acs.jced.5c00066 Read Online

ACCESS | Metrics & More | Article Recommendations | Supporting Information

ABSTRACT: The refractive indices of aqueous lithium bromide (LiBr−H_2O) solutions were measured over a wide range of mass fractions, from 0 to 0.62 kg/kg (62%), at seven wavelengths between 436.1 and 655 nm. Measurements were conducted over a temperature range of 296.15 to 320.15 K, with 1 K increments, using a commercial refractometer. In total, 3485 refractive index measurements were recorded, covering 35 compositions at 25 temperatures for each of the seven wavelengths. A parametrization model was proposed to unify the data set. The wavelength dependence of the refractive indices was further analyzed by using the Cauchy dispersion relation, from which three main coefficients were determined to predict $n(\lambda)$ for arbitrary wavelengths. Additionally, the optical contrast factors $\partial n/\partial T$ and $\partial n/\partial w$ were determined from the parametrized data. The effect of the surfactant (1-octanol) on the refractive index and contrast factors was carefully analyzed.

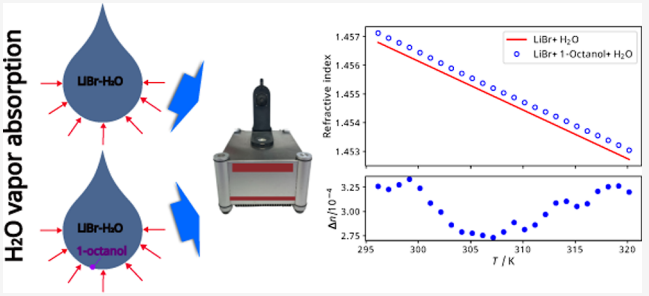

INTRODUCTION

Understanding the heat and mass transfer between absorbent solutions and vapor is critical for absorption refrigeration,[1] waste treatment,[2] air dehumidification, and pollutant absorption systems used in air and liquid purification, where absorbents trap pollutants.[3,4]

Aqueous lithium bromide solutions (LiBr−H_2O) are among the best choices as working fluids in absorption chillers, heat transformers, and refrigerating systems.[1,5] To achieve maximum efficiency, lithium bromide absorption chillers need to operate at a certain temperature and composition. It is therefore essential to determine the concentration of the solution at various locations as a function of temperature and time. A reliable and convenient method for measuring the concentration is through the refractive index, which can be obtained by either withdrawing a sample or, more invasively, in situ measurements within the system.

Advances in lasers and image processing techniques over the last few decades have enabled digital interferometry to drastically increase the accuracy of measurements. For monitoring concentration and temperature changes in transparent media, the interferometric approach is increasingly in demand[6,7] as it effectively correlates with their temporal changes. In absorption research, this is particularly useful for tracking system dynamics in the presence of a surfactant. The application of interferometric methods provides valuable insight into the performance and efficiency of a system but requires knowledge of the thermal and solutal contrast factors, which represent the derivatives of the refractive index with respect to temperature and concentration. Accurately measured contrast factors are essential for developing experimental techniques to study convection and heat and mass transfer in absorption and diffusive systems.

Although in situ composition tracking can be challenging, complementary numerical simulations[8−10] are highly useful in understanding the flow dynamics. For a meaningful comparison with the experimental data, it is often necessary to recalculate the numerical results into the optical phase, which also requires knowledge of the optical contrast factors.

The available data on the refractive index of LiBr are limited in both temperature and composition ranges.[11,12] In the range of compositions of practical interest, there appears to be a discrepancy in the dynamics of $n(w)$ behavior in these two sources. Here w is the mass fraction of LiBr in the binary mixture LiBr−H_2O. Furthermore, the existing data were obtained at a single wavelength, corresponding to the sodium

Received: February 7, 2025
Revised: May 15, 2025
Accepted: June 4, 2025

Table 1. Chemical Specifications as per the Suppliers

IUPAC name	abbreviation	molecular weights	CAS Reg. No	suppliers	purity	purification
Lithium bromide	LiBr	86.85	7550−35−8	Sigma-Aldrich Company	≥0.99 kg/kg	None
1-Octanol	CH3(CH2)7OH	130.23	111−87−5	Sigma-Aldrich Company	≥0.99 kg/kg	None
Deionized Water	H_2O	18.02	7732−18−5	Autwomatic Plus system of Wasserlab	conductivity <1 μS/cm	none

D line, m_D = 589.3 nm, which may not provide sufficient accuracy for comprehensive analysis across varying conditions.

This paper reports the refractive indices of LiBr solutions as a function of mass fraction up to 0.62 kg/kg (62%) over a temperature range of 296.15 to 320.15 K. Furthermore, refractive indices were measured at seven wavelengths. Optical contrast factors, $\partial n/\partial T$ and $\partial n/\partial w$, were calculated from the parametrized data. We also examined the Cauchy dispersion relation. In addition, the refractive indices of LiBr solutions in the presence of the surfactant octanol were measured. While small quantities of surfactants generally have a minimal impact on many physical properties, they can affect optical properties. The specific objective of this study is to provide data that will improve our understanding of the behavior of absorbent materials. These results significantly extend the database of this important absorbent.

EXPERIMENTAL METHODS

Solutions Preparation. The chemicals used in this study together with their basic information are summarized in Table 1. Given the extreme hygroscopic nature of lithium bromide, it is essential to follow a strict procedure to prevent unintentional absorption of moisture from the atmosphere during sample preparation. Lithium bromide (LiBr), with a mass fraction purity of ≥99% (CAS 7550−35−8), was obtained from Sigma-Aldrich Company. Before the samples were prepared, the LiBr was heated in an oven at 120 °C for a minimum of 16 h. Immediately after removal from the oven, LiBr was weighed directly into the sealed jar used for sample preparation to minimize exposure to atmospheric moisture.

A digital mass balance Gram VXI-310 was employed to measure both the LiBr and water masses with a combined standard uncertainty of ±0.0001 g. All solutions were prepared as mass fractions w [kg/kg] of anhydrous LiBr.

We prepared 35 solutions of different compositions covering the composition range from 0 up to w = 0.62 kg/kg.

Refractive Index Measurements. The data on refractive index, as well as the derived solutal and thermal contrast factors, were obtained using a multiwavelength Anton Paar Abbemat WR-MW refractometer. The apparatus was calibrated using distilled deionized water. Calibration was performed daily prior to measurements at the reference temperature of 298 K. The instrument's internal reference data, which are based on measurements relative to air, were used for this purpose. We verified that these internal values are consistent with the IAPWS formulation,[13] appropriately adjusted to the air reference frame. For each reported value, three individual measurements were collected and averaged. Before each measurement with a fresh solution, the apparatus was thoroughly cleaned with water and acetone. The mean values and standard deviations were calculated. The temperature of the sample and the internal temperature of the optical system were maintained within ±0.03 K due to the two built-in Peltier devices. The instrument operates at seven different wavelengths of visible light, covering the range of λ = 436−655 nm, ensuring a precision of $\pm 4 \times 10^{-5}$ nm.

Comparison with Available Results. Figure 1 presents a comparison between our experimental data at λ = 589.3 nm and the literature data reported by Zaltash[11] and Labra et al.[12] Our and Zaltash's data are taken at T = 298.18 K; Labra's data are not available at this temperature; instead, values for T = 293.15 K and T = 303.15 K are given. The comparison is given in terms of the dependence $n(w)$ and is in excellent agreement with the Zaltash data and consistent with the data of Labra et al..

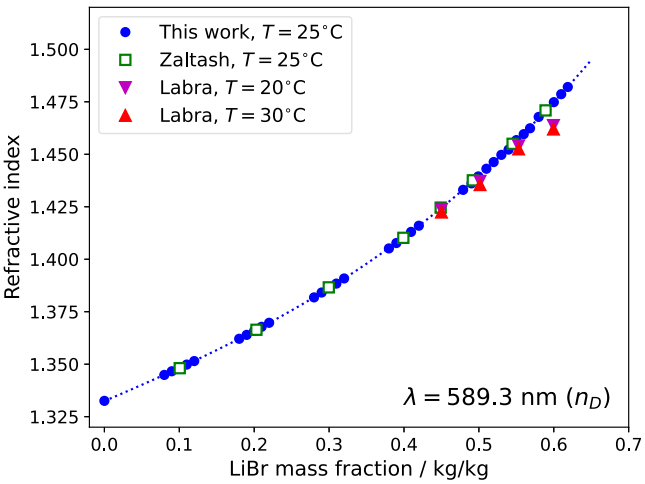

Figure 1. Comparison of measured data with literature values. This work - blue circles, values reported by Zaltash[11] - open green squares; values reported by Labra et al.[12] are given by magenta and red triangles. The dotted interpolation curve is for guidance only.

RESULTS AND DISCUSSION

Refractive Index of LiBr−H_2O Solutions. In this work, the experimental data of the refractive index (n) for the LiBr−water binary mixture were measured over the whole range of composition up to the saturation point, at temperatures from T = 296.15 K up to T = 320.15 K with a 1 K increment at 35 different compositions. The seven tables with raw data are given in Supporting Information.

Figure 2a presents the variation of the refractive index with temperature measured at different wavelengths of the composition of practical interest, w = 0.55 kg/kg. The general trend is a linear dependence when n decreases with an increase in temperature, which can be correlated using the following equation

$$n_\lambda(T) = a_\lambda^{00} + a_\lambda^{10} \times (T - T_0) \quad (1)$$

where a_λ^{00} and a_λ^{10} are adjustable parameters depending on wavelength and T_0 = 298.15 K. The slopes a_λ^{10}, which are associated with optical contrast factor $\partial n/\partial T$, weakly decrease from $a_\lambda^{10} = -1.73 \cdot 10^{-4}$ to $a_\lambda^{10} = -1.69 \cdot 10^{-4}$ as the wavelength

https://doi.org/10.1021/acs.jced.5c00066
J. Chem. Eng. Data XXXX, XXX, XXX−XXX

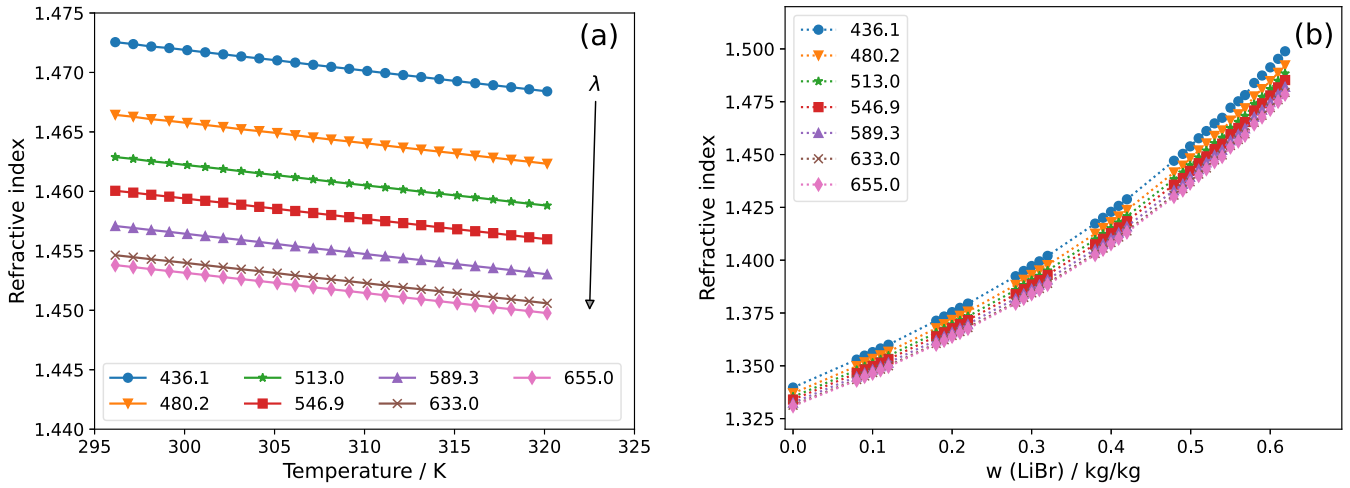

Figure 2. Experimental refractive indices. (a) Variation of refractive index with temperature measured at different wavelengths at w = 0.55 [kg/kg]; (b) variation of refractive index with mass fraction of LiBr measured at different wavelengths at T = 298.15 K. The curves are for guidance only.

varies from λ = 436 nm to λ = 655 nm. Note that these values are consistent only for a mass fraction w = 0.55 kg/kg.

Panel (b) shows the variation of the refractive index with the mass fraction of LiBr measured at different wavelengths at T = 298.15 K. It can be seen that the 35 compositions studied are divided into seven groups for convenience. The last three groups include continuous measurements, as this area is of particular interest for chillers. The raw data for one composition in each group, i.e., w = 0.1, 0.2, 0.3, 0.4, 0.5, 0.55, and 0.6 kg/kg are given as a single table (Tables S1−S7 in the Supporting Information) including the n values at 25 different temperatures and at seven wavelengths.

Unlike temperature, the composition dependence on the refractive index exhibits a third order polynomial behavior, which requires the determination of four adjustable coefficients for each temperature; see details in the next section. As can be seen from Figure 3, the refractive index decreases with wavelength. However, the effect is quite weak.

To extend the measured data to arbitrary wavelengths, we examine the dispersion relations between refractive index n and wavelength λ. Aqueous solutions are polar and inherit the strong absorption features of water in the infrared.[14,15] Our measurements include deep UV or IR and are made at a wavelength range of 455 nm ≤ λ ≤ 655 nm. Among the various dispersion equations, the Sellmeier and the Cauchy formula are the most common.[15] Careful analysis of molar refractivity of water and/or dilute water vapor in literature[14−16] provides the basis that the use of Cauchy equation in the form

$$n(\lambda) = A + \frac{B}{\lambda^2} + \frac{C}{\lambda^4} + \ldots \quad (2)$$

is justified in the considered range of wavelengths. Here A, B, and C are coefficients that can be determined by fitting them to the measured refractive indices.

We have calculated all three coefficients, and they can be found in the Supporting Information in the last columns of all seven tables.

Our previous studies of nonpolar mixtures[17,18] showed that adding the $1/\lambda^4$ to the Cauchy equation improves the accuracy of the interpolation by an order of magnitude with resulting MAPD (mean absolute percentage deviation) on the level of 0.002%.

$$\mathrm{MAPD} = \frac{1}{N}\sum_{i=0}^{N}\left|\frac{n_i^{\mathrm{exp}} - n_i^{\mathrm{fit}}}{n_i^{\mathrm{fit}}}\right| \times 100\% \quad (3)$$

Parameterization of the Measured $n_\lambda(w, T)$ Values. The temperature and concentration dependencies of refractive index $n_\lambda(T, w)$ were parametrized independently for each wavelength. The parametrization is done with the use of `statsmodels` library for Python programming language.[19] The raw data at all measured temperatures and concentrations were fitted to a polynomial equation of the following form

$$n_\lambda(T', w) = \sum_{i=0}^{N}\sum_{j=0}^{M} a_\lambda^{(ij)} T'^i w^j \quad (4)$$

where $T' = T - T_0$ is the temperature relative to the reference T_0 = 298.15 K. The highest polynomial orders N and M with respect to temperature and concentration, respectively, were found by analyzing the corresponding dependencies individually, using subsets with a constant second parameter. An example of the analysis is shown in Figure 4, where the plotted residues are calculated as

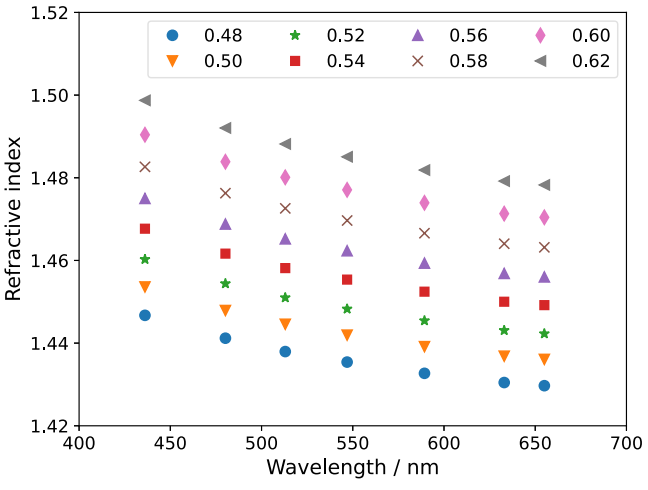

Figure 3. Variation of the refractive index with wavelength at T = 303.15 K for different mixture compositions [kg/kg], as indicated in the plot.

https://doi.org/10.1021/acs.jced.5c00066
J. Chem. Eng. Data XXXX, XXX, XXX−XXX

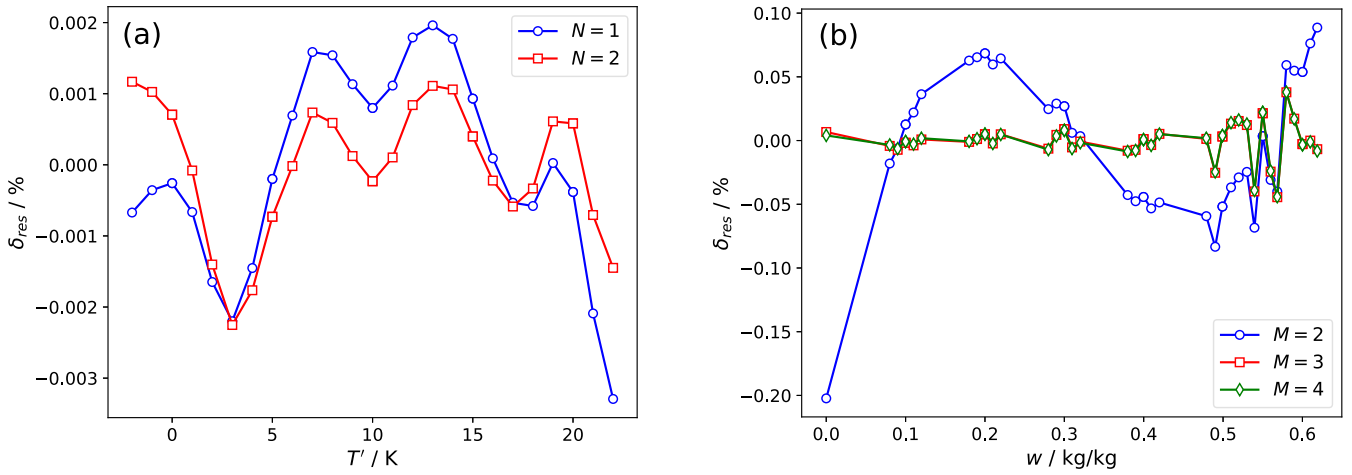

Figure 4. Selecting the highest orders of the polynomials N and M from a comparison of the residuals between the measured values and the fit to the data when either w or T are constant. (a) Temperature dependence of refractive index at 589.3 nm and w = 0.30 kg/kg. (b) Concentration dependence of refractive index at 589.3 nm and T = 308.15 K.

$$\delta_{\text{res}} = \frac{n_{\text{meas}} - n_{\text{fit}}}{n_{\text{fit}}} \times 100\% \tag{5}$$

As seen in Figure 2a, the temperature dependence of n_λ is close to linear. We tested the adequacy of the first-order polynomial by comparing it with the polynomial of the second-order (see Figure 4a for the results). This comparison demonstrates that the second order polynomial fitting does not provide an essential improvement in the accuracy; thus, the optimal polynomial order for the temperature dependence may be limited to N = 1.

It follows from Figure 2b that the dependence of n_λ on the concentration is nonlinear. To determine the most suitable polynomial fit, we tested polynomials of second and higher orders (see the comparison of the fits in Figure 4b). The polynomial of the second order is insufficient, while the polynomial of the fourth order does not improve the fit accuracy compared to the third order. Consequently, the optimal polynomial order for the concentration dependence was chosen as $M = 3$.

As a result, the final form of the data parametrization becomes

$$n_\lambda(T', w) = a_\lambda^{(00)} + a_\lambda^{(01)} w + a_\lambda^{(02)} w^2 + a_\lambda^{(03)} w^3 + a_\lambda^{(10)} T' + a_\lambda^{(11)} T' w + a_\lambda^{(12)} T' w^2 + a_\lambda^{(13)} T' w^3 \tag{6}$$

Alternatively, the eq 6 can be presented in the matrix form as

$$n_\lambda(T', w) = (1\,T') \times \begin{bmatrix} a_\lambda^{(00)} & a_\lambda^{(01)} & a_\lambda^{(02)} & a_\lambda^{(03)} \\ a_\lambda^{(10)} & a_\lambda^{(11)} & a_\lambda^{(12)} & a_\lambda^{(13)} \end{bmatrix} \begin{pmatrix} 1 \\ w \\ w^2 \\ w^3 \end{pmatrix} \tag{7}$$

Next, we examined a need in the higher order terms of eq 6, namely, the coefficients $a_\lambda^{(11)}$, $a_\lambda^{(12)}$, and $a_\lambda^{(13)}$. This is an essential step, as the presence of excessive terms may increase the uncertainty of the high-order coefficients. This analysis was done by comparing the fit results with all eight coefficients $a_\lambda^{(ij)}$ (hereafter 8-parameter fit), with removed $a_\lambda^{(13)}$ coefficient (7-parameter fit), with removed $a_\lambda^{(12)}$ and $a_\lambda^{(13)}$ coefficients (6-parameter fit), and with removed all three high-order coefficients $a_\lambda^{(11)}$, $a_\lambda^{(12)}$, $a_\lambda^{(13)}$ (5-parameter fit). The visualization and comparison of the fit results are convenient via the concentration dependence of the temperature contrast of the refractive index, $\partial n/\partial T$, presented in Figure 5.

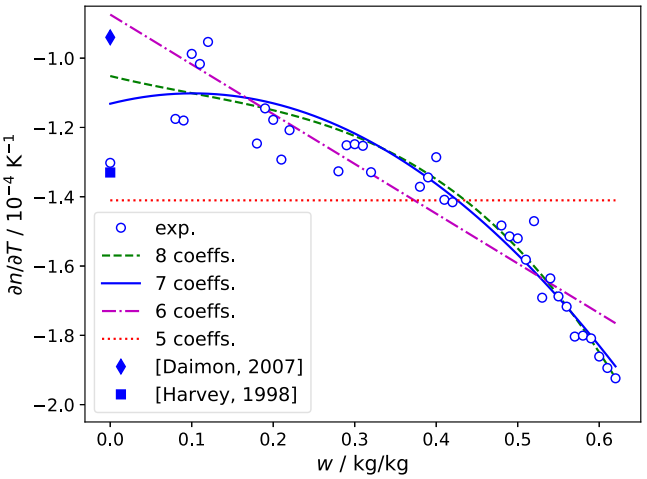

Figure 5. Comparison of the fit results with different numbers of high-order terms in the parametrization by eq 6 for the refractive index at 633 nm and T = 308.15 K. The literature data on the contrast factor of pure water are taken from ref 13 at 633 nm and 308.15 K and from ref 14 at 644 nm and 294.65 K.

The results of the different fits are presented in the plot by curves, while the experimental points are obtained by independent linear interpolation of the measurements at all assessed w_i.

Obviously, limiting the fit to 5 coefficients is not a good option, as it leads to $\partial n/\partial T$ = constant in the full concentration range. The fit with 6 coefficients provides a linear dependence $\partial n/\partial T = f(w)$, which is better but still does not outline the contrast factor behavior in diluted solutions. The 7-parameter fit bends the contrast factor dependence toward the literature data for pure water from refs. 13,14, which is also consistent with our own data. The dependence $n(T)$ for pure water is nonlinear in a wide temperature range; thus, for comparison with our results we selected the values specific to T = 308.15

https://doi.org/10.1021/acs.jced.5c00066
J. Chem. Eng. Data XXXX, XXX, XXX−XXX

Table 2. Coefficients of the Polynomial Parameterization of the Refractive Index of LiBr−Water Solutions in the Concentration Range of 0.0−0.60 Mass Fraction and the Temperature Range of 296.15 < T < 320.15 K at Seven Measured Wavelengths

	wavelength λ, nm						
Coeff	436.1	480.2	513.0	546.9	589.3	633.0	655.0
$a_\lambda^{(00)}$	1.33971	1.33692	1.33522	1.33390	1.33244	1.33120	1.33082
	(0.00009)	(0.00009)	(0.00009)	(0.00009)	(0.00009)	(0.00009)	(0.00009)
$a_\lambda^{(01)}/10^{-1}$	1.6118	1.5747	1.5554	1.5379	1.5224	1.5068	1.5047
	(0.0089)	(0.0086)	(0.0085)	(0.0084)	(0.0083)	(0.0082)	(0.0083)
$a_\lambda^{(02)}/10^{-1}$	0.499	0.460	0.433	0.419	0.394	0.386	0.369
	(0.027)	(0.026)	(0.026)	(0.026)	(0.025)	(0.025)	(0.025)
$a_\lambda^{(03)}/10^{-1}$	1.709	1.704	1.706	1.700	1.707	1.700	1.710
	(0.026)	(0.025)	(0.025)	(0.025)	(0.024)	(0.024)	(0.024)
$a_\lambda^{(10)}/10^{-4}$	−1.186	−1.170	−1.162	−1.141	−1.139	−1.132	−1.120
	(0.062)	(0.060)	(0.060)	(0.059)	(0.058)	(0.057)	(0.058)
$a_\lambda^{(11)}/10^{-4}$	0.74	0.67	0.65	0.57	0.59	0.59	0.57
	(0.41)	(0.40)	(0.40)	(0.39)	(0.39)	(0.38)	(0.39)
$a_\lambda^{(12)}/10^{-4}$	−3.15	−3.03	−3.00	−2.90	−2.92	−2.93	−2.93
	(0.58)	(0.57)	(0.56)	(0.55)	(0.55)	(0.54)	(0.55)
$a_\lambda^{(13)}/10^{-4}$	0	0	0	0	0	0	0
MAPD, %	0.0095	0.0093	0.0091	0.0090	0.0089	0.0087	0.0087

K, which is a middle of the temperature interval explored in the present work. The full 8-parameter fit does not improve the agreement between the experiment and the fit but even worsens the agreement for the low salt concentration. Consequently, we selected a 7-parameter fit as a working approach, which in practice means dropping the last term from the RHS of eq 6 or setting $a_\lambda^{(13)} = 0$ in eq 7.

The coefficients for fitting the data at different wavelengths are summarized in Table 2.

Refractive Index of LiBr−H_2O Solution in the Presence of Surfactant. Surfactants are used to enhance the absorption process.[20] In the presence of even a small disturbance, they cause additional surface tension gradients in the LiBr−water solution. These gradients, in turn, promote liquid motion near the interface, a phenomenon referred to as Marangoni convection.[9,10] Two common surfactants for LiBr aqueous solutions are 1-octanol and 2-ethyl-1-hexanol.

Hereafter, we denote the concentration of the surfactant as w_s. The optical properties of the LiBr−water system were studied with the addition of a small amount ($w_s \approx 140 - 170$ ppm) of 1-octanol (CAS 111−87−5) to solutions of LiBr−H_2O in the range of compositions w = 0.48−0.62 kg/kg and at temperatures of 298.15, 303.15, 308.15, 313.15, and 318.15 K. This range of LiBr mass fractions is of most practical interest. The uncertainty of the mass fraction of the surfactant is 0.066.

The experimental results are shown in Figure 6a in open circles. Measurements reveal that the addition of 1-octanol affects the refractive index of LiBr/H_2O solutions in a composition-dependent manner. The largest change in refractive index was observed at a LiBr mass fraction of w = 0.50 kg/kg, where the mean deviation, $\Delta n \sim 4.2 \times 10^{-4}$, was consistent across all seven wavelengths, corresponding to a change of about 0.008%.

However, comparing measurements directly between systems with and without the surfactant can be misleading due to small differences in the concentration of the basic LiBr/H_2O solutions used in each set of measurements. To minimize the influence of these outlier points, where some of the variation in Δn may be due to the LiBr concentration deviation rather than the surfactant, the measurements with surfactant

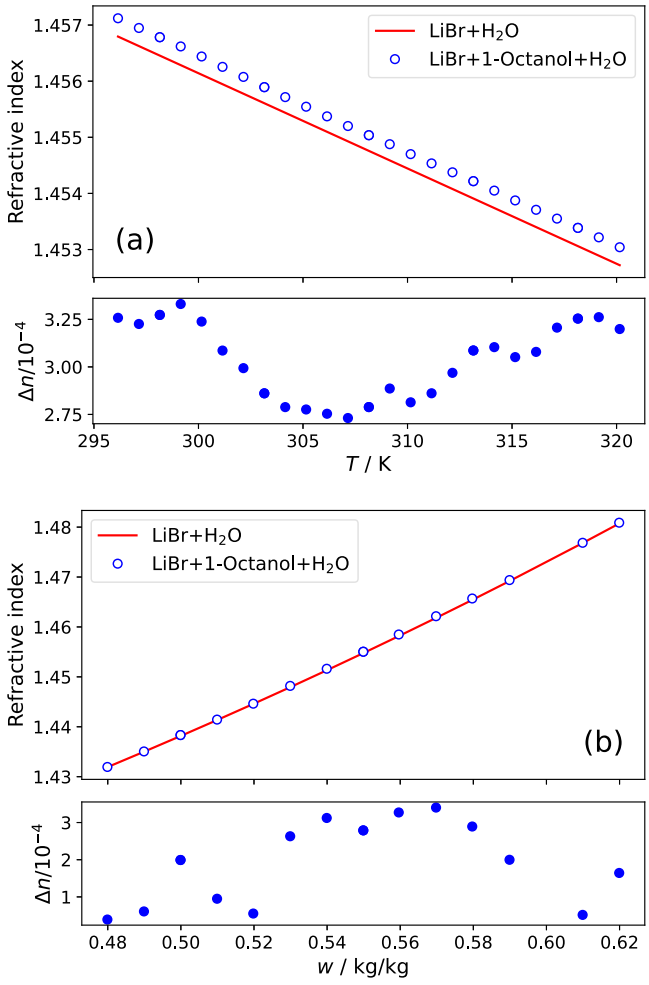

Figure 6. Refractive index in the LiBr−H_2O system with (1-octanol) surfactant and without (using eq 6) at λ = 589.3 nm and the difference Δn between them. (a) Temperature dependence at w = 0.55 kg/kg and (b) concentration dependence at T = 308.15 K.

https://doi.org/10.1021/acs.jced.5c00066
J. Chem. Eng. Data XXXX, XXX, XXX−XXX

are compared to the parametrized refractive index of the LiBr−water solution without 1-octanol, as given by eq 6.

Figure 6 presents a comparison of the refractive index values for LiBr−H_2O solutions with and without the surfactant, using the parametrized n values, along with the corresponding Δn caused by the surfactant at the bottom panel. This comparison confirms our suspicion regarding the compositional variation, as there is a small but noticeable difference between the parametrized refractive index values for $w = 0.55$; see the upper plot. This difference is not visible in Figure 6a. The parametrized values are smoother, and they show a nearly constant difference in refractive index between the solutions with and without surfactant for all studied compositions.

The analysis of Figure 6 shows that the effect of adding 1-octanol on the refractive index has a minor variation with temperature (see panel a) and a slightly stronger effect with the composition of the LiBr−water solutions (as seen in panel b).

Overall, excluding some outliers, across the covered range of T and w the surfactant additive gives a consistent positive deviation to the refractive index falling into the range $\Delta n = 0.5-3.3 \cdot 10^{-4}$.

Optical Contrast Factors. *Contrast Factors of LiBr−H_2O Solutions without Surfactant.* The expressions for the contrast factors can be obtained by differentiating eqs 6 or 7. The term $a_\lambda^{(13)} w^3$ is omitted, as discussed above. The thermal optical contrast factors are independent of temperature and exhibit a quadratic dependence on composition

$$\left.\frac{\partial n_\lambda}{\partial T}\right|_w = a_\lambda^{(10)} + a_\lambda^{(11)} w + a_\lambda^{(12)} w^2 \tag{8}$$

The solutal optical contrast factors exhibit a linear dependence on the temperature and a quadratic dependence on composition

$$\left.\frac{\partial n_\lambda}{\partial w}\right|_T = a_\lambda^{(01)} + 2 \times a_\lambda^{(02)} w + 3 \times a_\lambda^{(03)} w^2 + a_\lambda^{(11)} T' + 2 \times a_\lambda^{(12)} T' w \tag{9}$$

The advantage of the matrix representation of the parametrization is that the same matrix of the coefficients

$$[a_\lambda^{(ij)}] = \begin{bmatrix} a_\lambda^{(00)} & a_\lambda^{(01)} & a_\lambda^{(02)} & a_\lambda^{(03)} \\ a_\lambda^{(10)} & a_\lambda^{(11)} & a_\lambda^{(12)} & 0 \end{bmatrix} \tag{10}$$

can be used both for refractive index and the contrast factors calculation, with corresponding modification of the vectors of powers for T' and w, as follows

$$\left.\frac{\partial n_\lambda}{\partial T}\right|_w = (01)[a_\lambda^{(ij)}] \begin{pmatrix} 1 \\ w \\ w^2 \\ w^3 \end{pmatrix} \tag{11}$$

and

$$\left.\frac{\partial n_\lambda}{\partial w}\right|_T = (1T')[a_\lambda^{(ij)}] \begin{pmatrix} 0 \\ 1 \\ 2w \\ 3w^2 \end{pmatrix} \tag{12}$$

The contrast factors of LiBr−H_2O solutions, required for optical experiments, are shown in Figure 7 and are given in the

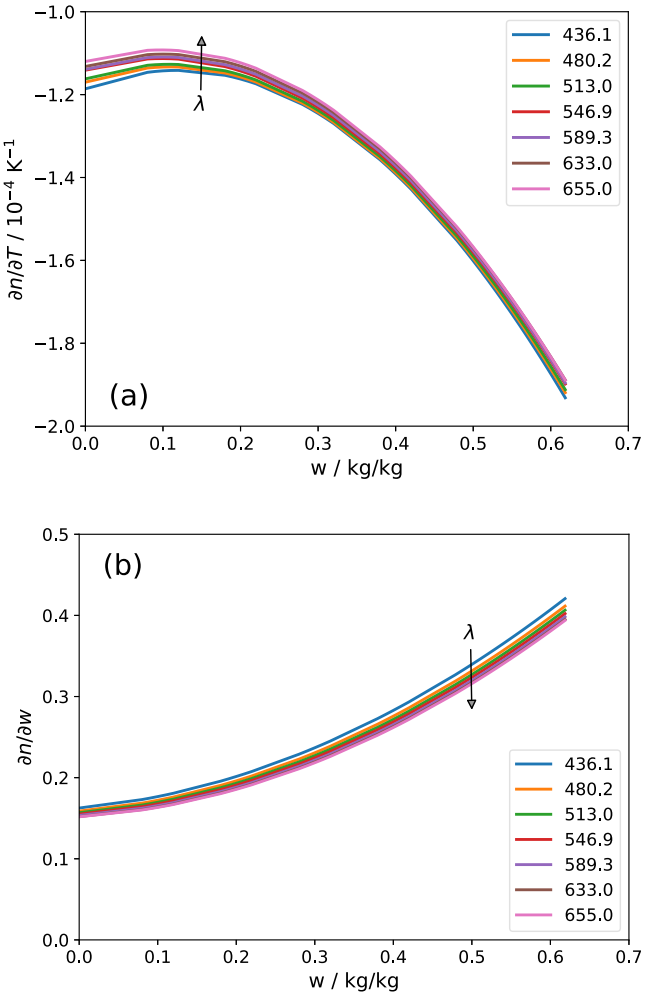

Figure 7. Variation of (a) thermal and (b) solutal contrast factors with LiBr mass fraction at seven wavelengths indicated in the plot at T = 298.15 K ($T' = 0$).

form of tables in the Supporting Information. They are calculated using eqs 8 and 9 with the parametrization coefficients listed in Table 1. Figure 7 illustrates that the dependence of the contrast factor on the wavelength is generally not significant. However, the thermal contrast factor $(\partial n/\partial T)$ exhibits a larger dependence on λ for lower mass fractions, while $\partial n/\partial T$ exhibits a larger dependence at higher mass fractions. Another observation is that $\partial n/\partial T$ decreases with w, whereas $\partial n/\partial w$ increases with w. It is important to note that $\partial n/\partial T$ is of the order of 10^{-4}, while $\partial n/\partial w$ is of the order of 1.

Contrast Factors of LiBr−H_2O Solutions with Surfactant 1-Octanol. Two approaches were applied to study how the surfactant affects the optical properties of the mixture. First, the influence of the surfactant on the thermal contrast factor was examined. Already looking at Figure 7a, one may anticipate a similar magnitude of $\partial n/\partial T$ for the mixtures without and with surfactant. This is confirmed by Figure 8, which summarizes the thermal contrast factor for both types of mixtures as a function of salt concentration, w, supporting the preliminary observation of their similarity.

https://doi.org/10.1021/acs.jced.5c00066
J. Chem. Eng. Data XXXX, XXX, XXX−XXX

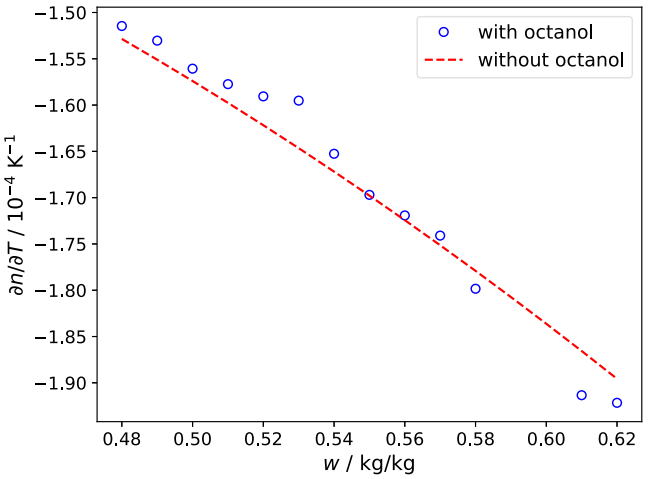

Figure 8. Variation of thermal contrast factor with LiBr mass fraction at 589.3 nm wavelength for the mixtures without and with surfactant.

Next, we sought to estimate the contrast factor of 1-octanol at infinite dilution as well as its potential dependence on temperature and concentration. The estimation of $\partial n/\partial w_s$ was conducted as follows: the refractive index excess due to the surfactant was calculated as the difference between the measured value for the mixture with surfactant and the parametrized value for the mixture without octanol, $\Delta n = n_{w+w_s}^{\mathrm{exp}} - n_w^{\mathrm{param}}$. The contrast factor was then determined by dividing the refractive index excess by the accurately measured concentration of 1-octanol.

$$\left.\frac{\partial n}{\partial w_s}\right|_{T,w} = \frac{\Delta n}{w_s} \tag{13}$$

While we did not parametrize the contrast factor $\partial n/\partial w_s$ over all assessed range of parameters, we estimated it for selected cases to gain a general understanding of its magnitude. The results are presented in Figure 9.

From the plot in Figure 9a, it can be observed that the temperature dependence of $\partial n/\partial w_s$ is very weak if present at all. In contrast, the concentration of basic salt w has a significant, nonlinear effect on the contrast factor, as shown in Figure 9b.

For the most relevant concentrations, the contrast factor at infinite dilution of w_s falls within the range of $\partial n/\partial w_s = 1 - 2$, which is 2 to 4 times higher than the maximum solutal contrast factor for the LiBr−H_2O solutions. This pronounced optical effect of 1-octanol is expected due to its large and heavy molecular structure. However, the measured contrast factor for octanol is still several times lower compared to that of polymer solutions.

CONCLUSIONS

The study provides a comprehensive data set of 6125 refractive index measurements for aqueous LiBr solutions across a wide range of compositions, temperatures, and wavelengths. In addition to the measured values of n at seven wavelengths, the coefficients for the Cauchy dispersion relation were carefully determined, offering a reliable method to predict the refractive index for arbitrary wavelengths. The measured refractive index data were parametrized, improving the utility of the data and minimizing the impact of outliers.

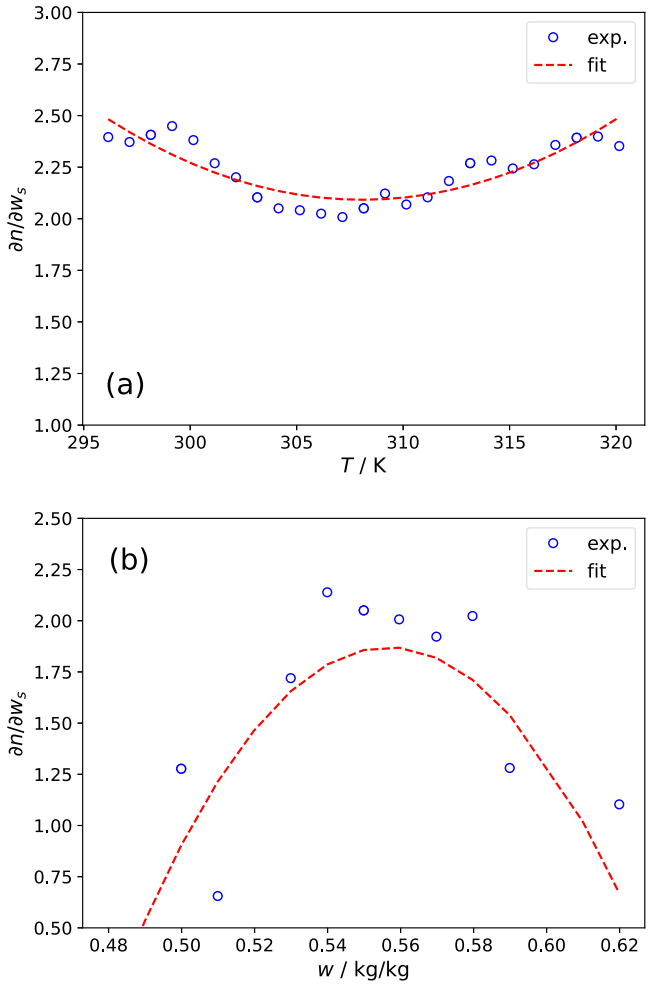

Figure 9. Solutal contrast factor of 1-octanol at infinite dilution in the LiBr−H_2O mixture at λ = 589.3 nm. (a) Temperature dependence at w = 0.55 kg/kg and (b) concentration dependence at T = 308.15 K.

The optical contrast coefficients, $\partial n/\partial T$ and $\partial n/\partial w$, calculated from the parametrized data provide important information about the temperature and concentration dependencies of the refractive index. This may be of importance for optical and thermophysical applications, such as heat transfer and concentration gradient processes involving LiBr solutions.

The effect of the surfactant (1-octanol) on the refractive index and contrast factors was also carefully analyzed. Additionally, we determined the contrast factors of 1-octanol at an infinite dilution.

ASSOCIATED CONTENT

Supporting Information

The Supporting Information is available free of charge at https://pubs.acs.org/doi/10.1021/acs.jced.5c00066.

Thermal ($\partial n/\partial T$) and solutal ($\partial n/\partial w$) contrast factors of LiBr− H_2O solutions at T = 298 K; refractive indices of LiBr− H_2O solutions and Cauchy coefficients for mass fractions w = 0.1, 0.2, 0.3, 0.4, 0.5, 0.55, and 0.60 kg/kg at temperature range 295 K ≤ T ≤ 320 K; and refractive indices of LiBr− H_2O with the addition of surfactant, 150 ppm of 1-octanol, at temperature range 295 K ≤ T ≤ 320 K (PDF)

All measured data (3485 points) (XLSX)

https://doi.org/10.1021/acs.jced.5c00066
J. Chem. Eng. Data XXXX, XXX, XXX−XXX

AUTHOR INFORMATION

Corresponding Authors

Aliaksandr Mialdun − *Fluid Mechanics Group, Faculty of Engineering, Mondragon University, 20500 Mondragon, Spain;* orcid.org/0000-0002-7787-2865; Email: amialdun@mondragon.edu

Peru Arroiabe − *Fluid Mechanics Group, Faculty of Engineering, Mondragon University, 20500 Mondragon, Spain;* orcid.org/0000-0002-8103-8777; Email: parroiabe@mondragon.edu

Ane Errarte − *Fluid Mechanics Group, Faculty of Engineering, Mondragon University, 20500 Mondragon, Spain;* orcid.org/0000-0002-7451-0711; Email: aerrarte@mondragon.edu

Valentina Shevtsova − *Fluid Mechanics Group, Faculty of Engineering, Mondragon University, 20500 Mondragon, Spain; Ikerbasque, Basque Foundation for Science, Bilbao 20500, Spain;* orcid.org/0000-0001-6109-5048; Email: x.vshevtsova@mondragon.edu

M. Mounir Bou-Ali − *Fluid Mechanics Group, Faculty of Engineering, Mondragon University, 20500 Mondragon, Spain;* orcid.org/0000-0003-1491-1182; Email: mbouali@mondragon.edu

Author

Irene Pérez de Luco − *Fluid Mechanics Group, Faculty of Engineering, Mondragon University, 20500 Mondragon, Spain*

Complete contact information is available at: https://pubs.acs.org/10.1021/acs.jced.5c00066

Notes

The authors declare no competing financial interest.

ACKNOWLEDGMENTS

The work is supported by Elkartek program (KK-2023/00041-MMASINT) and Research Group Program (IT1505-22) of the Basque Government and Grant PID2021-124232OB-I00 (Treated, AEI/FEDER, UE) funded by MCIN/AEI/10.13039/501100011033 of the Spanish Government and, as appropriate, by "ERDF A way of making Europe", by the "European Union".

REFERENCES

(1) Best, R.; Rivera, W. A review of thermal cooling systems. *Appl. Therm. Eng.* **2015**, *75*, 1162−1175.

(2) Engelpracht, M.; Gibelhaus, A.; Seiler, J.; Graf, S.; Nasruddin, N.; Bardow, A. Upgrading Waste Heat from 90 to 110°C: The Potential of Adsorption Heat Transformation. *Energy Technol.* **2021**, *9*, 2000643.

(3) Beal, C.; Gardner, E.; Menzies, N. Process, performance, and pollution potential: A review of septic tank-soil absorption systems. *Aust. J. Soil Res.* **2005**, *43*, 781.

(4) Xie, J.; Wang, D.; Liu, L.; Shao, T.; Zhou, H.; Zhang, D. An Overview of Flue Gas SO2 Capture Technology Based on Absorbent Evaluation and Process Intensification. *Ind. Eng. Chem. Res.* **2024**, *63*, 6066−6086.

(5) Arshi Banu, P.; Sudharsan, N. Review of water based vapour absorption cooling systems using thermodynamic analysis. *Renew. Sust. Energy Rev.* **2018**, *82*, 3750−3761.

(6) Köhler, W.; Mialdun, A.; Bou-Ali, M. M.; Shevtsova, V. The Measurement of Soret and Thermodiffusion Coefficients in Binary and Ternary Liquid Mixtures. *Int. J. Thermophys.* **2023**, *44*, 140.

(7) Shevtsova, V.; Köhler, W.; Bou-Ali, M. M.; Mialdun, A. Progress in multicomponent thermodiffusion studies in connection with the DCMIX space experiments. *Chem. Phys. Rev.* **2024**, *5*, 031307.

(8) Arroiabe, P.; Martinez-Agirre, M.; Bou-ali, M. M. Numerical analysis of different mass transfer models for falling film absorbers. *Int. J. Heat Mass Transfer* **2022**, *182*, 121892.

(9) Arroiabe, P. F.; Martinez-Agirre, M.; Nepomnyashchy, A.; Bou-Ali, M. M.; Shevtsova, V. The effect of small perturbation on dynamics of absorptive LiBr−water solution. *Phys. Fluids* **2024**, *36*, 022119.

(10) Arroiabe, P. F.; Martinez-Agirre, M.; Nepomnyashchy, A.; Bou-Ali, M. M.; Shevtsova, V. Marangoni-driven pattern formation in an absorbing binary mixture. *Phys. Fluids* **2024**, *36*, 0000.

(11) Zaltash, A.; Ally, M. R. Refractive indexes of aqueous lithium bromide solutions. *J. Chem. Eng. Data* **1992**, *37*, 110−113.

(12) Labra, L.; Juárez-Romero, D.; Siqueiros, J.; Coronas, A.; Salavera, D. Measurement of properties of a lithium bromide aqueous solution for the determination of the concentration for a prototype absorption machine. *Appl. Therm. Eng.* **2017**, *114*, 1186−1192.

(13) Harvey, A. H.; Gallagher, J. S.; Sengers, J. M. H. L. Revised Formulation for the Refractive Index of Water and Steam as a Function of Wavelength, Temperature and Density. *J. Phys. Chem. Ref. Data* **1998**, *27*, 761−774.

(14) Daimon, M.; Masumura, A. Measurement of the refractive index of distilled water from the near-infrared region to the ultraviolet region. *Appl. Opt.* **2007**, *46*, 3811−3820.

(15) Kedenburg, S.; Vieweg, M.; Gissibl, T.; Giessen, H. Linear refractive index and absorption measurements of nonlinear optical liquids in the visible and near-infrared spectral region. *Opt. Mater. Express* **2012**, *2*, 1588−1611.

(16) Zeiss, G.; Meath, W. J. The H2O-H2O dispersion energy constant and the dispersion of the specific refractivity of dilute water vapour. *Mol. Phys.* **1975**, *30*, 161−169.

(17) Mialdun, A.; Shevtsova, V. Analysis of multi-wavelength measurements of diffusive properties via dispersion dependence of optical properties. *Appl. Opt.* **2017**, *56*, 572−581.

(18) Errarte, A.; Schraml, M.; Köhler, W.; Shevtsova, V.; Bou-Ali, M. M.; Mialdun, A. Thermophysical, Optical, and Mass Transport Properties of C60 Fullerene Solutions in Toluene and Tetralin. *J. Chem. & Engng Data* **2022**, *67*, 2160−2173.

(19) Seabold, S.; Perktold, J. Statsmodels: Econometric and Statistical Modeling with Python. In *Proceedings of the 9th Python in Science Conference*, 2010; pp 92−96.

(20) Ziegler, F.; Grossman, G. Heat-transfer enhancement by additives. *Int. J. Refrigeration* **1996**, *19*, 301−309.